

Review

# A Review on the Removal of Heavy Metals from Water by Phosphorus-Enriched Biochar

Yang Zeng<sup>1</sup>, Yuhan Lin<sup>1</sup>, Ming Ma<sup>1,2,3</sup> and Hong Chen<sup>1,2,3,\*</sup><sup>1</sup> College of Resources and Environment, Southwest University, Chongqing 400715, China<sup>2</sup> Chongqing Engineering Research Center for Agricultural Non-Point Source Pollution Control in the Three Gorges Reservoir Area, Chongqing 400715, China<sup>3</sup> Chongqing Key Laboratory of Agricultural Resources and Environment, Chongqing 400715, China

\* Correspondence: chenhong@swu.edu.cn

**Abstract:** In recent years, the utilization of phosphorus-enriched biochar (PBC) has attracted significant attention due to its exceptional stability and surface reactivity. This review systematically summarizes the advancements in research related to the application of PBC as an adsorbent for remediating water contaminated with heavy metals. Initially, the precursors utilized in the production of PBC, encompassing biomass and phosphorus sources, are introduced. Subsequently, the distinct physicochemical properties and adsorption characteristics resulting from phosphorus doping on the biochar surface through various carbonization processes and parameters are elucidated. Additionally, the diverse adsorption mechanisms employed by PBC in removing heavy metals from water are analyzed. Lastly, future research prospects and associated challenges concerning PBC are presented. This paper aims to furnish comprehensive background information for the practical implementation of PBC in the purification of heavy metal-contaminated water environments.

**Keywords:** phosphorus-rich biochar; precursor; carbonization process; adsorption mechanism



**Citation:** Zeng, Y.; Lin, Y.; Ma, M.; Chen, H. A Review on the Removal of Heavy Metals from Water by Phosphorus-Enriched Biochar. *Minerals* **2024**, *14*, 61. <https://doi.org/10.3390/min14010061>

Academic Editor: Eric D. van Hullebusch

Received: 17 November 2023

Revised: 18 December 2023

Accepted: 24 December 2023

Published: 4 January 2024



**Copyright:** © 2024 by the authors. Licensee MDPI, Basel, Switzerland. This article is an open access article distributed under the terms and conditions of the Creative Commons Attribution (CC BY) license (<https://creativecommons.org/licenses/by/4.0/>).

## 1. Introduction

With the rapid advancement of industry, agriculture, and a significant surge in urbanization, an abundance of bioavailable and readily accessible heavy metals are being discharged into the environment through various human activities such as mineral extraction, combustion of fuels, wastewater irrigation, utilization of fertilizers and pesticides, and vehicular emissions [1]. These heavy metals possess enduring toxicity, a propensity for bioaccumulation, and exhibit remarkable resistance to degradation. Consequently, they infiltrate the soil and water ecosystems either through direct release or indirect sedimentation, resulting in their concentrations surpassing the natural background levels. It leads to irreversible harm across all levels of the food chain and significantly affects human health and ecosystem stability [2,3]. Hence, it is imperative to urgently explore technologies aimed at remediating water pollution caused by heavy metals and ensuring the safety of water quality.

Currently, various physical, chemical, and biological methods have been applied to purify heavy metals in water. However, the heterogeneous nature of pollution levels, and the different types of pollution, significantly compromise the effectiveness of these remediation approaches [4]. Among these methods, adsorption has emerged as a promising technique due to its exceptional ability to remove and immobilize heavy metals in the environment. Consequently, numerous materials, including biomaterials [5], nanomaterials [6], mineral materials [7], and carbon-based materials [8], have garnered attention as potential adsorbents. Notably, biochar, characterized by its high porosity and remarkable persistence, has found widespread application in the treatment of both inorganic and organic pollutants [9]. By further modifying its properties, such as the specific surface area (SSA) and abundance of surface functional groups, the adsorption capacity of biochar for heavy metals in water

can be enhanced [10,11]. Various modification techniques are employed, including physical modification (steam, ball milling, etc.), corrosive modification (acid-base, oxidation, etc.), and doping modification (ion, heteroatom, etc.) [12]. Of particular interest is the preparation of PBC, which significantly enhances its conductivity, thermal stability, and the number of active surface sites, finding broad applications in electrochemistry, catalysis, and adsorption, among other fields [13–15].

Phosphorus represents a fundamental element that exerts a significant impact on both industry and agriculture, serving as a critical non-renewable strategic resource. However, the excessive exploitation of phosphate deposits has led to their gradual depletion on a global scale [16]. Consequently, it has become crucial to optimize phosphorus input, enhance phosphorus utilization efficiency, mitigate soil phosphorus losses, alleviate water eutrophication, and minimize the phosphorus losses resulting from human activities during the phosphorus cycle [12]. One noteworthy avenue for achieving sustainable phosphorus utilization involves the efficient and environmentally friendly recovery of phosphate-rich waste materials. Unfortunately, these valuable resources are often underutilized, resulting in phosphorus losses and a range of environmental pollution issues [17]. For instance, the improper incorporation of straw into fields can increase the risk of pests and diseases, reduce plant emergence rates, and the uneven mixing of straw with soil can lead to diminished soil permeability, thus causing reductions in crop yield and quality [18]. Directly applying manure to the soil facilitates the reclamation of essential nutrients, thereby enhancing soil fertility. However, the portion that exceeds the soil and plant absorption capacity is lost through various channels, including surface runoff, leaching, and volatilization, thereby leading to phosphorus accumulation in soil and water eutrophication [19]. While sludge holds substantial potential as a phosphorus source, it cannot be directly discharged or applied to the environment due to its potential content of inorganic pollutants (high salinity, multiple heavy metals), organic pollutants (pharmaceuticals, hormones, halogenated hydrocarbons), and other harmful substances, including pathogens (pathogens, viruses, insect eggs) [20]. Consequently, enhancing phosphorus conversion efficiency and mitigating environmental risks during the recycling of phosphorus-rich waste materials have become critical areas of research.

The utilization of heat treatment to mitigate the toxicity and concentration of phosphorus-rich waste has become the prevailing approach, offering several advantages. First, heat treatment possesses universal applicability as it can effectively treat precursors from diverse sources with varying characteristics [21]. Second, the process parameters of heat treatment can be tailored to produce a range of target products such as carbon black, tar, and combustible gas, enabling the recovery of multiple forms of energy [22]. Third, the heat treatment process facilitates the decomposition of organic pollutants and microorganisms, leading to a reduction in water content and in the volume of the precursor, thereby achieving a harmless reduction effect [23]. Lastly, heat treatment serves as a means of concentrating available elements, thus enabling the complete recycling of phosphorus-rich waste [24]. Furthermore, the conversion of phosphorus-rich waste to PBC through heat treatment offers the added advantage of stable phosphorus loading onto the biochar. The incorporation of phosphorus, as a heteroatom, significantly enhances the adsorption capabilities of biochar, broadening its potential applications [25]. Consequently, through heat treatment, phosphorus-rich waste not only addresses the issue of solid waste management but also yields an environmentally friendly and functional carbon-based material capable of addressing heavy metal concerns and facilitating waste treatment.

In this section, several representative reviews, including phosphorus conversion processes during biomass pyrolysis, the preparation of PBC, and its environmental applications in remediation of soil heavy metals are presented to provide an overview of recent research progress. Huang et al. [26] explores the alterations in phosphorus form and availability under various treatment conditions. They further discuss the advantages and disadvantages of different analytical techniques such as  $^{31}\text{P}$  NMR, XANES, XRD, Hedley protocol, and improved methodologies. Another review by Peiris et al. [27] focuses on the types

of precursors and preparation methods used for PBC, highlighting the advantages of using PBC in soil remediation and its mechanism for immobilizing heavy metals. Chen et al. [28] summarized the application of PBC in different environmental aspects, and systematically reviewed the migration and transformation mechanism of phosphorus in the thermochemical treatment of various solid wastes.

In summary, phosphorus holds significant functional value in biochar. PBC exhibits exceptional properties that make it well-suited for use as an adsorbent. However, previous reviews did not delve into the effects of different phosphorus sources and carbonization processes on phosphorus conversion within PBC. Additionally, they fail to provide a comprehensive and in-depth discussion on the environmental application of PBC in addressing water pollution caused by heavy metals, or the adsorption mechanisms involved. Therefore, the objective of this paper is to: (1) review the impacts of various precursors (including endogenous phosphorus in biomass, exogenous phosphorus in additives) as well as different preparation methods and parameters, on the phosphorus form and availability of PBC; (2) review the adsorption mechanism of PBC for heavy metals in water environments; and (3) present a summary of the challenges and development prospects associated with PBC, accompanied by suggestions for further research.

## 2. Phosphorus in PBC

### 2.1. Precursor and Endogenous Phosphorus

Numerous studies utilize phosphorus-rich materials as biochar precursors for pyrolysis without the need for additional additives. In this case, the phosphorus of the resulting PBC solely comprises the endogenous phosphorus present within the biomass. The quantity and form of this endogenous phosphorus are contingent upon the selection of the biomass, including factors such as the type of biomass, the source and form of phosphorus within the biomass, and other influential factors. These factors collectively contribute to the heterogeneity observed in the properties of PBC. Biochar precursors, serving as carriers of phosphorus, can be categorized into three groups: plant-derived waste, animal-derived waste, and sewage sludge. Plant-derived waste can be further divided into agricultural by-products containing cellulose and hemicellulose as the primary components, as well as forestry waste predominantly composed of lignin. Animal-derived waste encompass mixtures such as poultry feces, bedding materials, livestock feces, and animal residues. Sewage sludge is classified based on different processes and stages [29].

Phosphorus in plant-derived waste is transformed by plants into free inorganic orthophosphate groups (including orthophosphate, pyrophosphate, and polyphosphate) or organophosphate compounds (such as monophosphate, diphosphate,  $\alpha$ - and  $\beta$ -glycerophosphate, and organic polyphosphate) through the absorption of  $\text{HPO}_4^{2-}$  and  $\text{H}_2\text{PO}_4^-$  from the soil. The content and proportion of these compounds in plants are determined by factors such as plant species, varieties, growth stages, and organs [30].  $^{31}\text{P}$  NMR analysis of phosphorus forms in plant-derived waste reveals that organophosphorus accounts for 40%–70% of the total extractable phosphorus [26]. Feed materials like crop seeds and bran contain a significant amount of phosphorus in the form of phytic acid phosphorus (60%–80%). The varying utilization of phytic acid in the feed of different animal species contributes to the heterogeneity of phosphorus content in feces. Furthermore, different way of rearing (distributed and intensive) and the use of feed additives (such as inorganic phosphate and phytase) also lead to differences in manure phosphorus content [31]. Animal residues, with representatives such as animal bones and fish scales as calcium and phosphorus precursors, and seafood shells as calcium precursors, serve as crucial raw materials for the thermal synthesis of hydroxyapatite [32]. Phosphorus in sewage sludge primarily originates from untreated sewage and chemical agents added during the treatment process. Untreated sewage contains microorganisms and organic compounds with phosphorus from diverse sources. The phosphorus in activated sludge, produced through biological dephosphorization, mainly exists in the form of organic phosphorus, such as polyphosphate within the cells of phosphorus-accumulating bacteria. Conversely, chemically enhanced primary

sludge, generated through chemical dephosphorization, exhibits higher levels of inorganic phosphorus, primarily in the form of Al-P and Fe-P [33]. The concentration of endogenous phosphorus in dynamic wastes and sewage sludge, expressed as a proportion of dry weight (ranging from 0.58% to 3.74% and 1.58% to 4.88%, respectively), is significantly higher than that in plant wastes (ranging from 0.05% to 0.89%) [28,34].

## 2.2. Additives and Exogenous Phosphorus

The addition of exogenous phosphorus can greatly enhance the adsorption properties of biochar. There are two common types of added phosphorus sources: water-soluble phosphates and insoluble phosphate minerals, which have different solubilities. Both types of phosphorus sources act as suppliers of phosphorus, promoting the carbonization of biochar to achieve increased carbon storage [28].

Water-soluble phosphates are frequently used as pore activators, promoting the dehydrogenation and depolymerization of biomass during the pyrolysis process to form biochar materials rich in mesoporous and microporous structures. Moreover, phosphorus from water-soluble phosphates is doped at the edge plane sites of the carbon lattice as a heteroatom. This allows it to function as an active site and electron donor, significantly enhancing the adsorption of heavy metal anions such as Cr (VI) and As (V) [35]. Phosphates like  $K_3PO_4$  are often employed in microwave-assisted pyrolysis to produce PBC, which serves multiple roles as a microwave absorbent, catalyst, and phosphorus precursors. These PBC products are characterized by a high micropore surface area, cation exchange capacity, and phosphorus content, rendering them excellent adsorbents for water heavy metals and soil modifiers [36,37].

Insoluble phosphate minerals, such as hydroxyapatite (HAP) and chlorapatite (ClAP), are loaded onto the biochar template to prevent the aggregation of mineral particles with high surface energy and provide active sites. This enhances the surface adsorption and chemical precipitation properties of biochar [38,39]. The impregnation of biomass with phosphate tailings, with calcium fluorophosphate as the primary component, can also slightly increase the SSA and the number of functional groups in biochar [40].

The addition of additives not only introduces different forms of exogenous phosphorus but also influences the physical and chemical properties of PBC in the presence of metal and non-metal ions. Alkali metal and alkaline earth metal ions (Ca(II), Mg(II), K(I), Na(I)) are the most common Lewis acids associated with the incorporation of exogenous phosphorus into biochar. On the one hand, they act as catalysts, promoting the thermal decomposition of polymers and improving the pore structure of biochar. On the other hand, by adjusting the proportion of additives, the content of non-apatite inorganic phosphorus (NAIP) can be increased, or highly bioavailable hydroxyapatite (HAP) can be formed to maximize phosphorus recovery [33].

The addition of additives containing ammonium salts, such as  $NH_4H_2PO_4$ ,  $(NH_4)_3PO_4$ , can hinder the pore development of biochar, sometimes reducing the SSA of PBC to levels even lower than that of the original biochar [41]. This could be due to the rapid release of ammonia and other volatile small molecules during the formation of biochar pores, leading to increased pressure and collapse of the pore structures [42]. However, the SSA of PBC prepared by Li et al. [43] using ammonium phosphate and coffee shells was as high as  $1133\text{ m}^2\text{ g}^{-1}$ . This discrepancy may be due to the different production processes of direct pyrolysis and staged pyrolysis. In staged pyrolysis, the temperature is initially raised to a lower temperature and maintained for a period to remove organic matter and avoid the influence of ammonia gas on the pore structure.

When halogen ( $Cl^-$ ) is introduced at a low temperature (873 K), PBC with uniform nano@ClAP on its surface can be synthesized to efficiently remove heavy metal cations by ion exchange [44]. Additionally, the Cl additive can combine with heavy metals in sludge-based biochar, reducing the heavy metal content in the product through the volatilization of heavy metal chloride at high temperatures ( $>1173\text{ K}$ ). Simultaneously, more soluble phosphate-containing crystals, such as ClAP, are formed, which convert lead ions into

more stable precipitates of lead chlorophosphate [44] However, under high-temperature conditions (1373 K), CIAP is prone to solid deoxidation reactions with carbon in biomass, resulting in the volatilization of reduced phosphorus into the gas phase and a decrease in the phosphorus retention rate of biochar [45].

In particular, plant-derived wastes can also be used as calcium source additives to enhance the amount of mobile and bioavailable phosphorus phases in sludge-based biochar, thereby stabilizing endogenous heavy metals [46]. Thomas et al. [47] used FactSage to calculate thermodynamic equilibrium and proved that the main phosphorus compound in biochar was potassium phosphate through the introduction of  $K^+$  from plant-derived waste instead of calcium phosphate, iron phosphate and aluminum phosphate, resulting in more plant-available phosphorus in the product. However, in practical applications, the formation of amorphous phosphates (such as  $Ca_3(PO_4)_2$  and  $(AlPO_4)$ ) through non-equilibrium phase transformation cannot be ignored, as they may lead to differences between the actual results and the expected calculation results.

### 3. Carbonization Process and Influencing Parameters

Pyrolysis methods targeting biochar as the main product can be categorized into conventional pyrolysis (CPS) and hydrothermal carbonization (HTC). Their products are respectively pyrochar and hydrochar, both of which are collectively referred to as biochar. Microwave-assisted pyrolysis (MCPS), microwave-assisted hydrothermal carbonization (MHTC) and solar-assisted pyrolysis, which are different from traditional pyrolysis energy sources, have gradually become research hotspots. Solar pyrolysis, in particular, offers advantages such as sustainability and high heat flux density [48]. However, there have been limited reports on the combination of solar pyrolysis with PBC. As a result, this paper focuses on investigating the effects of CPS, HTC, MCPS, MHTC, as well as their respective parameters, on the preparation of PBC.

#### 3.1. Conventional Pyrolysis

CPS refer to the dry heat treatment of biomass under conditions of inert gas or limited oxygen, resulting in the production of pyrochar. Various parameters, such as pyrolysis temperature, atmosphere, and residence time, have been extensively studied for their influence on the migration and transformation of phosphorus. During anoxic pyrolysis, organophosphorus compounds begin to undergo pyrolysis at relatively low temperatures (523 K), leading to the gradual dominance of pyrophosphate (Pyro-P) in the temperature range of 573–873 K. Subsequently, as the temperature increases (>973 K), Pyro-P transforms further into orthophosphate (Ortho-P) [49].

Xu [50] demonstrated that pyrolysis temperature is the primary factor determining phosphorus stability using the Hedley protocol, as well as solid-phase and liquid-phase  $^{31}P$  NMR. Additionally, as an inorganic mineral element, phosphorus continues to accumulate in pyrochar over prolonged residence times (<2 h), with the total phosphorus content gradually increasing until it reaches stability [51]. The pyrolysis atmosphere ( $N_2$ ,  $CO_2$ ) mainly affects the yield and SSA of pyrochar, while its impact on phosphorus transformation is relatively minor [52]. The elemental composition of the precursor, including the form and content of phosphorus and metal ion content, has been identified as a determinant of phosphorus retention rate and form in phosphorus-rich pyrochar.  $H_2O$ -P and Olsen-P decrease significantly with the phase transition, such as dehydration and crystallization, of inorganic phosphorus. Furthermore, organophosphates or polyphosphates tend to combine with metal ions or mineral components after thermal decomposition. Hence, the content of different metal ions in the precursor influences the fluidity and bioavailability of phosphorus to a certain extent. For example, the abundance of NaOH-P is positively correlated with the content of Fe(II) and Al(II), while the abundance of HCl-P is positively correlated with the content of Ca(II) [26].

The principle of MCPS is to generate internal friction heat inside the biomass through dipole and interface polarization and the ion conduction effect, which can reduce the

reaction temperature and greatly shorten the pyrolysis time. The local hot spots formed can promote the graphitization of biochar and reduce the influence of secondary cracking gas on the formation of pores. At the same time, the hot-spot effect enhances the reactive activity and improves the stability of the C-P chemical bond to increase phosphorus storage in pyrochar, so that the structural defects caused by loading more phosphorus atoms are an important reason for the increase of surface active sites and SSA on phosphorus-rich pyrochar [13]. Similar to traditional pyrolysis, energy input intensity (pyrolysis temperature, microwave power) determines the total phosphorus (TP) content of phosphate-rich pyrochar from the sludge source. Higher energy input intensity also facilitates the conversion of most of the organic phosphorus (OP) in the sludge into inorganic phosphorus (IP). Non-apatite inorganic phosphorus (NAIP) is transformed into apatite inorganic phosphorus (AIP) with lower bioavailability [20,53]. A large number of studies in the literature have applied microwave to the preparation of biochar from sludge, which is due to the fact that water in sludge is a polar molecule that enhances the microwave absorption capacity, while many types of biomass are not sensitive to microwave radiation [54]. Therefore, due to the complex physical and chemical properties of biomass raw materials (moisture, structure, microwave absorption capacity), achieving higher selectivity and improved functional pyrolysis products relies on striking a balance between microwave parameters and selecting suitable microwave absorbents and catalysts.

### 3.2. Hydrothermal Carbonization

HTC refer to the wet heat treatment of biomass under low reaction temperatures, using water as the reaction medium and self-generated pressure within a closed system. In comparison to CPS, HTC is considered a more favorable approach for recovering resources from phosphorus-rich biomass, such as manure, sludge, and aquatic plants, which typically have high water contents. HTC enables the production of PBC in a gentler and more energy-efficient way by reducing the reaction temperature [55]. Subcritical water facilitates various reactions in biomass, including decarboxylation, dehydration, hydrolysis, condensation, polymerization, and aromatization. Phosphorus is transformed along with these reaction processes, and the transformation process can be divided into three steps:

1. 323–433 K, intracellular or extracellular phosphate-containing compounds are transformed into soluble phosphates such as phosphate monoester or Al-P, Fe-P, Ca-P through a complex process, and most of the former are released into the liquid phase rather than deposited in the solid phase;
2. 393–453 K, the phosphate monoester is completely converted into inorganic phosphorus in the liquid phase. The proportion of soluble inorganic phosphorus compounds entering the liquid phase increases;
3. >453 K, inorganic phosphorus present in the liquid phase undergoes a reaction with metal ions released from the biomass. This reaction leads to the formation of metal-associated phosphorus or insoluble phosphate that becomes loaded onto the hydrochar [56,57].

The influencing factors of phosphorus conversion in the above process can be divided into external factors, such as hydrothermal temperature and residence time, and internal factors such as precursor components and pH. For instance, Cui et al. [58] compared the fitting results of different HTC parameters with the total phosphorus in hydrochar derived from different wetland plants. They concluded that the precursor had a stronger impact on phosphorus retention in the products than the hydrothermal temperature. Chen et al. [28] cited this perspective and concluded that the main reasons for the influence of the precursor on phosphorus distribution were internal factors such as the initial distribution of phosphorus forms and the concentration of metal cations present in the biomass. External factors not only directly impact the morphological changes of phosphorus but also indirectly influence its transformation by altering internal factors. For instance, the hydrothermal temperature can affect the degree and rate of degradation of macromolecular organic matter in the precursor. This degradation process produces acidic substances like organic

acids and phenolic compounds, which decrease the pH and promote the transformation from AIP to non-apatite inorganic NAIP and from OP to IP [57,59]. As the hydrothermal temperature continues to rise, the degradation products further decompose, leading to the generation of alkaline substances such as ammonium ions. This gradual increase in alkalinity tends to neutralize the pH [23]. Additionally, the hydrothermal temperature determines the leaching rate of metal cations, which can have a synergistic effect with the final pH and collectively impact the retention of phosphorus in hydrothermal carbon [60].

MHTC does not appear to have a significant effect on the conversion trends of endogenous phosphorus. Shi et al. [61] compared the form and concentration of phosphorus in solid products of MHTC and HTC at different temperatures and at the same duration using the SMT protocol and P XANES spectrum. The study found no significant difference, except for a slightly better phosphorus promotion and preservation effect observed at a reaction temperature of 443 K. However, previous literature has demonstrated that MHTC offers more efficient energy input, significantly shortens the reaction time, and produces hydrochar with better pore distribution and activity [62]. This suggests that the precursor and reaction medium undergo more drastic changes under microwave conditions [61]. Thus, more studies are needed to verify the conversion mechanism of biomass and phosphorus in the MHTC process due to these contradictory results.

#### 4. PBC Adsorbs Heavy Metals in Water

##### 4.1. Advantages and Research Status of PBC as Adsorbent

PBC has been extensively studied as an effective adsorbent for the treatment of heavy metal wastewater due to its remarkable adsorption capabilities (Table 1, Figure 1). It also shows great potential in the adsorption of multi-metal wastewater and in the selective adsorption of nuclides [63]. Moreover, PBC exhibits excellent cyclic adsorption capacity [43,64] and has a low eutrophication risk [65]. To further enhance its adsorption performance, researchers have explored the preparation of composite materials by incorporating nZVI, LDH, molybdenum disulfide ( $\text{MoS}_2$ ), and Gram-negative bacteria (GNB) onto PBC. These auxiliary components can be uniformly loaded onto the surface of PBC. In addition, the collaborative treatment of heavy metals in sewage is achieved through the mechanisms of reduction, precipitation, and biomimetic mineralization [66–69].

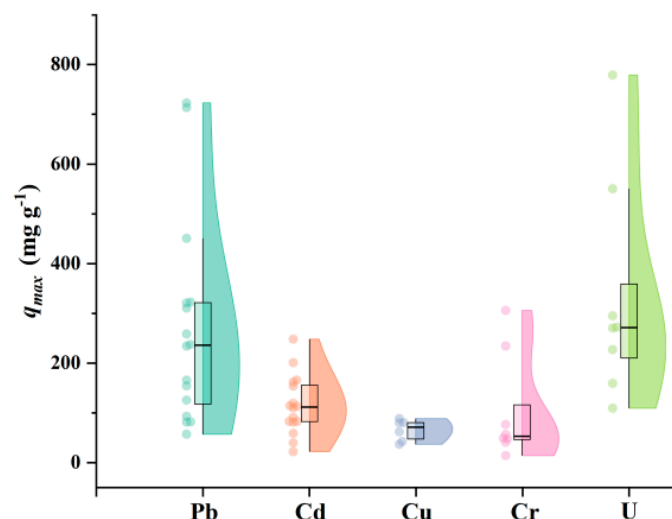


Figure 1. Raincloud plots of the maximum adsorption capacity of PBC for typical heavy metals.

Table 1. Reports about adsorption capacities of heavy metals by PBC.

HMs	PBC Precursor	Adsorption Conditions	$q_{\max}$ ( $\text{mg g}^{-1}$ )	Biochar Features on Adsorption	Ref.
Pb	Camellia oleifera shells, ( $\text{NH}_4, \text{H}$ ) <sub>n</sub> $2\text{P}_n\text{O}_{3n+1}$	C0: 100–2000 $\text{mg L}^{-1}$ , dose = 1 $\text{g L}^{-1}$ , pH = 6, T = 298 K, t = 360 min	723.6	High surface area and pore volume, rich P- and N-containing functional groups	[70]
	Bamboo sawdust, $\text{C}_6\text{H}_{18}\text{O}_{24}\text{P}_6$	C0: 50–300 $\text{mg L}^{-1}$ , dose = 0.4 $\text{g L}^{-1}$ , pH = 5, T = 293 K, t = 1440 min	234.8	Low ZPC, great surface modification (maximum of 2.1 wt% of P),	[63]
Cd	Raw bamboo scraps, $\text{K}_3\text{PO}_4 \cdot 3\text{H}_2\text{O}$	C0: 10–500 $\text{mg L}^{-1}$ , dose = 1 $\text{g L}^{-1}$ , pH = 6.8, T = 298 K, t = 720 min	249.8	Great pore structure (mainly micropores), high aromatization and graphitization, more P compounds (mainly $\text{PO}_4^{3-}$ and $\text{P}_2\text{O}_7^{4-}$ )	[37]
	Apple tree branches, $\text{K}_3\text{PO}_4 \cdot 3\text{H}_2\text{O}$	C0: 2–250 $\text{mg L}^{-1}$ , dose = 1 $\text{g L}^{-1}$ , pH = 6, T = 298 K, t = 1440 min	114.7	Higher P, C retention and electron density, High absolute value of zeta potential	[71]
Cu	Sewage sludge, $\text{CaCl}_2, (\text{NH}_4)_2\text{HPO}_4$	C0: NM, dose = 1 $\text{g L}^{-1}$ , pH = 5, T = 298 K, t = 1440 min	90.0	More dispersed HAP, High P loading	[39]
	Wood waste, $\text{CaCl}_2 \cdot 2\text{H}_2\text{O}$ , $\text{Na}_3\text{PO}_4 \cdot 12\text{H}_2\text{O}$	C0: 2–200 $\text{mg L}^{-1}$ , dose = 0.5 $\text{g L}^{-1}$ , pH = 7, T = 298 K, t = 1440 min	63.8	More inserted chlorophosphates, very small amount of AP	[65]
Cr	Oil-tea shells, $\text{H}_3\text{PO}_4$ , PEI/Methanol, Glutaraldehyde	C0: 200–600 $\text{mg L}^{-1}$ , dose = 1 $\text{g L}^{-1}$ , pH = 2, T = 313 K, t = 1440 min	320.5	More N- and P- containing groups that can act as electron donors (P also acts as adsorption sites of Cr and the adhesive sites of PEI); multi-scales and hierarchical with micro-, meso- and macropores	[35]
	<i>Egeria najas</i> , $\text{H}_3\text{PO}_4$ , $\text{FeSO}_4/\text{PEG}/\text{KBH}$	C0: 30–100 $\text{mg L}^{-1}$ , dose = 0.75 $\text{g L}^{-1}$ , pH = 5.5, T = 333 K, t = 1440 min	57.5	More dispersed nZVI, stronger antioxidant capacity (addition of $\text{H}_3\text{PO}_4$ )	[72]
U	Bamboo chopsticks, $\text{H}_3\text{PO}_4$ , citric acid	C0: 25–300 $\text{mg L}^{-1}$ , dose = 0.6 $\text{g L}^{-1}$ , pH = 4, T = 298 K, t = 100 min	781.0	Great affinity and selectivity for U (P-O, P=O provide a lone electron-pairs to form coordination bonds)	[73]
	Bamboo, $\text{KH}_2\text{PO}_4$ , $\text{AlCl}_3 \cdot 6\text{H}_2\text{O}$ , $\text{MgCl}_2 \cdot 6\text{H}_2\text{O}$	C0: 5–250 $\text{mg L}^{-1}$ , dose = 1 $\text{g L}^{-1}$ , pH = 4, T = 298 K, t = NM	274.2	High amounts of functional groups and ions (reduction and complexation: P-O, Mg-O-H and -OH, co-precipitation: polyhydroxy aluminum cations)	[66]

Note: The data selection criteria in the table are the scholarly papers corresponding to the best  $q_{\max}$  and the median value of the box plot. PEI = Polyetherimide, PEG = Polyetherimide, NM abbreviation stands for Not Mentioned.

#### 4.2. Adsorption Mechanism of PBC on Heavy Metals Wastewater

The potential mechanisms of heavy metal adsorption by PBC in water include mineral precipitation, ion exchange, functional group complexation, electrostatic interaction, physical adsorption, cation- $\pi$  interaction, and redox (Figure 2b). Cui [74] proposed that the contributions of ion exchange and mineral precipitation to adsorption can be determined by comparing the amount of heavy metals adsorbed by PBC and the net release of alkali metal cations before and after demineralization. The contributions of functional group complexation can be determined by comparing the pH changes before and after adsorption of heavy metals by demineralized PBC (DPBC). Zhang [75] suggested that the contributions of physical adsorption and electrostatic adsorption can be determined by oscillating saturated biochar in ultra-pure water and 0.01 M  $\text{NaNO}_3$  solution, respectively, to remove the physically adsorbed heavy metals. The difference in adsorption between the two cases can then be calculated to determine the contribution of the cation- $\pi$  bond (Figure 2a). Based

on this, studies have shown that the highest adsorption contribution in the original biochar is typically attributed to ion exchange, while mineral precipitation or ion exchange in PBC accounts for the highest adsorption contribution [39,71,76,77].

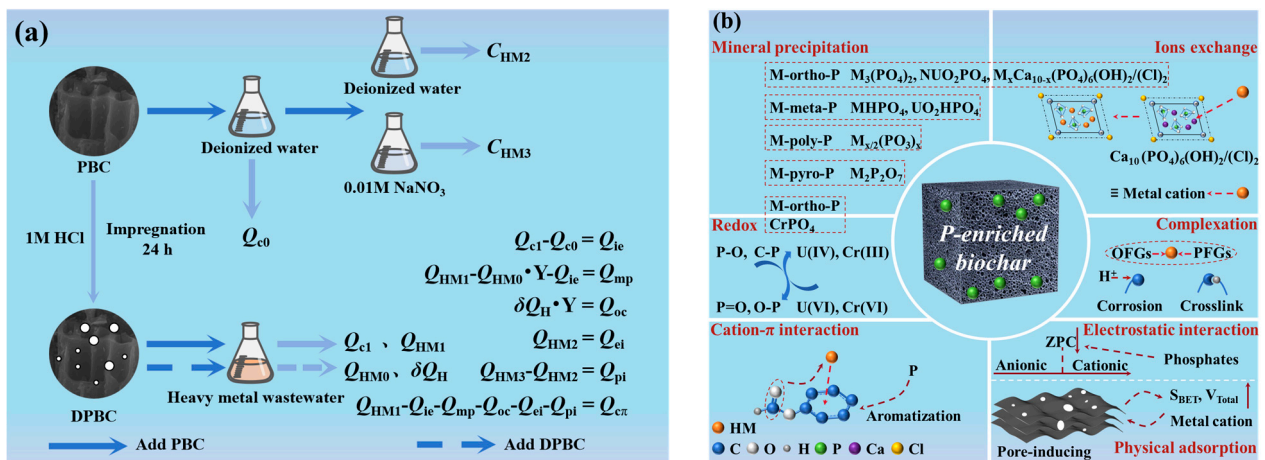


**Figure 2.** Quantitative method (a); and schematic diagram (b) of contribution of each mechanism to heavy metal adsorption. Note:  $C_{c1,2}$  represents the cation (K(I), Na(I), Ca(II) and Mg(II)) concentration after the adsorption of heavy metals,  $C_{HM0,1}$  represents the concentration of the adsorbed heavy metals,  $C_{HM2,3}$  represents the concentration of desorbed heavy metals,  $\delta C_H$  represents the net release concentration of hydrogen ions before and after adsorption,  $Q_{ie}$ ,  $Q_{mp}$ ,  $Q_{oc}$ ,  $Q_{ei}$ ,  $Q_{pi}$  and  $Q_{c\pi}$  represent the concentration of adsorbed heavy metals contributed by ion exchange, mineral precipitation, functional group complexation, electrostatic interaction physical adsorption, cation- $\pi$  interaction and other mechanisms, respectively. M represents Cd(II), Pb(II), Cu(II) and Zn(II), N represents K(I), Na(I).

#### 4.2.1. Mineral Precipitation

Phosphate, due to its strong binding affinity for heavy metals and provision of reaction sites, plays a crucial role in the stable binding of heavy metals to the surface of biochar through various phosphate precipitates. Consequently, the introduction of phosphorus transforms mineral precipitation into the primary mechanism for metal adsorption in PBC [78]. The specific form of phosphorus derived from different phosphorus precursors determines the types of precipitates formed, including ortho-P metal precipitates, meta-P metal precipitates, pyro-P metal precipitates, and poly-P metal precipitates [37,65,71,79].

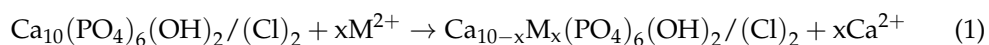
The solubility of the precipitates is an important indicator for assessing the competitive adsorption capacity of heavy metals. Cu(II) and Cd(II) exhibit strong competitive adsorption, whereas the competitive adsorption between Pb(II) and Cd(II) is relatively weak. This can be attributed to the lower solubility of lead orthophosphate and the similar solubility of copper and cadmium orthophosphates. The preferential precipitation of lead ions can hinder the ion exchange process between copper, cadmium, and PBC [65,80]. Furthermore, some studies have suggested that low concentrations of Cu(II) or Cd(II) can enhance the adsorption of Pb(II). However, as the concentration increases, Cu(II) or Cd(II) will compete with Pb(II) for adsorption sites, resulting in a reduction of the adsorption capacity of Pb(II) [65,80].

#### 4.2.2. Ion Exchange

Compared with the original biochar, PBC can improve the ion exchange capacity through two ways: one is to load HAP or CIAP functional materials, and the other is to incorporate alkali metals and alkaline earth metals as exchangeable cations when introducing exogenous phosphorus. The cations formed on the surface of PBC exchange ions with heavy metal ions in the solution and adsorb heavy metals (Equations (1) and (2)). By examining the concentration of K(I), Na(I), Ca(II) and Mg(II), or the characteristic peak

intensity of cations before and after the adsorption of heavy metals, we can ascertain the occurrence of ion exchange [39]. Liu [80] observed that the reflection peak underwent a displacement towards a higher diffraction angle subsequent to the adsorption of Cu(II) and Cd(II). This phenomenon could potentially be attributed to the ingress of Cu(II) and Cd(II) into the hydroxyapatite (HAP) lattice via an ion exchange process with Ca(II), subsequently resulting in a reduction in the size of the crystal unit cell. Moreover, the pyrolysis process induces alterations in the binding form of phosphorus and cation of the precursor, leading to enhancements in the overall dissolved concentrations of Ca(II) and Mg(II), as well as the slow-release effect. Consequently, PBC acquires a heightened and more enduring capacity to adsorb heavy metals through the mechanism of ion exchange [81].

The adsorptive characteristics of PBC under varying ionic strengths serve as crucial parameters for evaluating its efficacy in diverse application scenarios. The introduction of Na(I), Ca(II), and Mg(II) augments the ionic strength, resulting in the formation of a hydration layer on the biochar's surface. It increases steric hindrance and intensifies competition for available adsorption sites, ultimately leading to a decline in the adsorption capacity for heavy metal ions [41,82]. The ion strength significantly associated with adsorption capacity can prove the mechanism underlying the capture of heavy metal ions is governed by either ion exchange or outer-sphere complexation. Conversely, if the correlation is absent, it substantiates that the primary mode of heavy metal adsorption onto the surface of PBC is through inner-sphere complexation [73]:



#### 4.2.3. Surface Complexation

During the reaction process, the phosphorus precursor undergoes cross-linking with the organic carbon present in the biomass, facilitating the grafting of phosphorous groups. The released  $\text{H}^+$  ions then etch the surface of the biomass, leading to the formation of oxygen-containing functional groups. The increased abundance of these functional groups enhances the surface complexing capability of PBC [83]. By comparing the XPS and FTIR results of PBC before and after adsorption, it is evident that the binding energy associated with O-P-O and P=O decreases, accompanied by a shift in the absorption peak. This substantiates the involvement of phosphorus-containing groups in the adsorption process of heavy metals [41].

In practical applications, the presence of organic matter in water bodies can also influence the adsorption performance of PBC. This influence is often simulated using humic acid. Under acidic conditions, the adsorption of negatively charged humic acid by PBC becomes challenging due to electrostatic repulsion. Additionally, humic acid in solution readily forms complexes with heavy metals, thereby impeding the complexation process of heavy metals [63].

#### 4.2.4. Electrostatic Interaction

The electrostatic interaction between heavy metals and PBC is influenced by pH and zeta potential. When the pH exceeds the point of zero charge (ZPC), deprotonation results in a negatively charged surface on the PBC, allowing for the capture of heavy metal cations through electrostatic interaction [73]. As the pH increases, the absolute value of the zeta potential also increases, leading to an enhanced attraction between PBC and positively charged heavy metal cations. However, a continuous rise in pH can cause a shift in the dominant form of heavy metals in the aqueous solution. For instance, when the pH exceeds 8, uranium (VI) components primarily exist as negatively charged ions or complexes such as  $(\text{UO}_2)_3(\text{OH})_7^-$  and  $\text{UO}_2(\text{OH})_3^-$ . Due to the weak Coulombic effect, the electrostatic adsorption performance of PBC diminishes [73], and divalent heavy metals also gradually precipitate as hydroxides [39].

When the pH is below the ZPC, the surface becomes protonated and positively charged, resulting in the rejection of heavy metal cations through electrostatic repulsion. Additionally,  $H^+$  and  $H_3O^+$  ions in the solution may compete with heavy metal adsorption, limiting the adsorption process [65]. Furthermore, the introduction of phosphate on the surface of PBC can lower the ZPC value and further enhance the electrostatic effect [63,79]. Additionally, the charge, electronegativity, and ionic radius of heavy metals are closely linked to their competitive adsorption capacity on the surface of PBC. Under the same charge density, electronegativity determines the ability of heavy metals to be adsorbed through electrostatic forces, while the ionic radius governs the steric hindrance experienced by heavy metals during adsorption on the surface and within pores [76,84].

#### 4.2.5. Physical Adsorption

Higher temperatures and the addition of phosphorus serve to facilitate the vaporization of low-molecular organics, increase the SSA and total pore volume. However, a continuous rise in temperature can result in the collapse of mesopores or an increase in the degree of graphitization, which is not conducive to the formation of mesopores and macropores. Phosphate compounds can form cross-links with the carbon framework of biomass to mitigate the risk of pore collapse during pyrolysis [85]. Simultaneously, phytic acid,  $H_3PO_4$ , and other phosphate compounds, can serve as sources of  $H^+$  ions. In addition, pore-inducing elements, introduced alongside exogenous phosphorus, such as metals, alkaline earth metals,  $NH_4^+$ , and others, can collectively participate in the process of biomass carbonization. Their presence catalyzes the decomposition of organic matter, resulting in gas generation, and facilitating the formation of micropores [33,41]. Enhancing the pore structure and fostering synergistic effects among pores of varying scales provide additional pathways for the physical adsorption and diffusion of heavy metals, augmenting the phosphorus load on the surface of biochar and within its pores [71,83].

Additionally, the exchange of metal ions with water and their coordination to form hydrated ions occurs in solution. When the radius of hydrated ions exceeds the pore radius of PBC, the adsorption of heavy metals is restricted due to size limitations. Typically, the process requires dehydration for them to enter the interior of the pores. The rate of water exchange serves as an indicator for assessing the acquisition and loss of coordination water by heavy metals, which is influenced by ionic hydration energy. The magnitude of ionic hydration energy and the rate of water exchange are determined by the ionic radius and charge of the metal ions involved [86]. In general, smaller ionic radii and charges result in higher water exchange rates, lower ionic hydration energy, and stronger disparities between water and competitive adsorption capacities [87,88]. In general, ions with a smaller radius and higher charge exhibit a higher water exchange rate, lower ion hydration energy, stronger de-coordination water, and competitive adsorption capacity. The relevant data of the competitive adsorption of typical heavy metals are shown in Table 2.

**Table 2.** Influence parameters of the competitive adsorption of heavy metals [76,84,87,88].

Heavy Metal Ion	Atomic Electronegativity (Pauling)	Ionic Radius	Hydrated Radius	Hydration Energy kJ/mol	Hydrolysis Constant
		Å			
Pb	2.33	1.19	4.01	1481	7.71
Cu	1.90	0.73	4.10	2100	10.10
Cd	1.69	0.95	4.26	1828	7.70
Zn	1.65	0.74	4.30	2056	9.00

Note: The ionic radius depends not only on the ion charge and electron distribution, but also on the structure of the ionic compound (such as the coordination number, etc.). The above data are the ionic radius under the condition that the coordination number of heavy metals is equal to 6.

#### 4.2.6. Cation- $\pi$ Interaction

The cation- $\pi$  bond primarily involves a short-range non-covalent interaction between the delocalized  $\pi$  electrons provided by aromatic rings and unsaturated groups (such as

C=C, C=O, etc.) and heavy metals. This interaction leads to a reduction in the electron cloud density around the unsaturated group and an increase in its binding energy [39,89]. The incorporation of phosphorus further enhances the aromatization of PBC compared to the original biochar and improves its ability to act as an electron donor [41]. The intensity of characteristic peaks of the aromatic C-H bond and the H/C value are crucial indicators for evaluating the degree of aromatization [73,77].

It is important to note that the cation- $\pi$  interaction between biochar and different heavy metals varies. According to the soft and hard acid-base theory (HSAB), the strength of the interaction follows the order of soft acid (Cd(II)) > exchange acid (Cu(II), Zn(II), Pb(II)) > soft base (the aromatic structure of biochar). This rule provides a qualitative description of the difficulty, speed, and stability of the reaction products between these entities [90]. However, Chen et al. [39] drew a conclusion that contradicted the empirical rule. By comparing the characteristic peak intensity of the C=C group after the adsorption of Cu(II) and Cd(II), it was observed that the adsorption of the Cu(II) group showed more significant changes, implying that the cation- $\pi$  interaction may selectively favor Cu(II). To delve deeper, Zhao et al. [91] used DFT calculations to compare the contributions of cation- $\pi$  interaction and complexation to the adsorption of Cu(II) and Pb(II). The study revealed that the adsorption of Cu(II) through interaction bonding was stronger, while the opposite trend was observed for Pb(II).

#### 4.2.7. Redox

In PBC, grafted phosphate ions can serve as electron donors, inducing redox reactions with heavy metals. This process reduces the toxicity of heavy metals and enhances their removal through synergistic mechanisms. It has been observed that, after adsorbing U(VI) on PBC, the U(VI):U(IV) ratio in the solution is 8:5, indicating the involvement of magnesium and phosphate groups in the reduction of U(VI) [66]. Similarly, studies have shown that when PBC adsorbs Cr(VI) under acidic conditions, the binding energy of P-O and C-P decreases, while the proportion of P=O and O-P increases. The direction of electron transfer suggests that the phosphorus groups may act as electron donors in the reduction process of Cr(VI) [43]. Under low-pH conditions, Cr(VI) is adsorbed on the positively charged surface of PBC biochar in the form of  $\text{HCrO}_4^-$ . It is then converted into  $\text{CrPO}_4$  through reduction and precipitation [35,43]. The phosphate groups and carboxyl groups in PBC act as proton donors to maintain the proton consumption during the reduction of Cr(VI), thereby keeping the pH in a lower range. This provides a larger redox potential for the reduction of Cr(VI) [92]. Moreover, the introduction of phosphate can also inhibit the oxidation of auxiliary components, such as nZVI, loaded onto PBC, thereby achieving effective synergistic treatment in composite materials [93].

## 5. Challenge and Prospects

While PBC exhibits great potential as an adsorbent, there are still challenges and considerations for the theoretical research and practical application of PBC. Developing biochar with better cost efficiency and improved pore distribution while maintaining its adsorption performance is crucial. Additionally, addressing pollution in the production chain of PBC and potential secondary pollution during its use are important challenges. Indeed, the adsorption performance of raw biochar derived from different biomass sources is often unsatisfactory, prompting the addition of phosphorus sources through impregnation co-pyrolysis or post-pyrolysis impregnation to enhance the adsorption capabilities of PBC. However, the typical refined water-soluble phosphorus sources used in this process are obtained through the concentration and purification of medium- and low-grade phosphate ores, which are upstream products in the production chain of PBC. The pollution generated during the preparation process, including tailings, waste gas, and wastewater, can offset some of the environmental benefits associated with PBC. It is crucial to explore more environmentally friendly alternatives to external phosphorus sources. Therefore, medium- and low-grade phosphate ores appear to hold more potential as additional phosphorus

sources. These ores offer advantages, such as wide availability, cost-effectiveness, and a high content of mineral elements (such as K, Na, Ca, Mg, Si, P), that can enhance the adsorption capacity of PBC. Hence, the utilization of medium- and low-grade phosphate ores as phosphorus sources may be more compatible with the concept of “treating waste with waste” and promote a more comprehensive phosphorus cycle, which is beneficial for environmental sustainability.

Moreover, PBC can serve as a template for loading auxiliary components, leading to the formation of composite materials that further enhance application performance. However, it is imperative to verify whether phosphorus and auxiliary components undergo mutual consumption. It is essential to prevent them from competing at the loading sites on biochar. This can be accomplished by controlling the form and solubility of phosphorus or by modifying the carbonization process and the order in which phosphorus sources are added. By doing so, we can ensure a synergistic effect between phosphorus and auxiliary components, resulting in improved adsorption of heavy metals in water bodies.

Simultaneously, it is necessary to explore methods to enhance the phosphorus retention rate or grafting rate in various carbonization processes to achieve greater phosphorus utilization and improved recycling performance. A more systematic study is required to understand the trends and influencing factors associated with the transformation of phosphorus forms and availability. This can be achieved through the construction of models that simulate the evolution process and elucidate the mechanisms underlying the interaction between biomass and phosphorus.

Indeed, numerous studies have highlighted the potential of PBC in various environmental applications, including its use as a soil passivator, amendment, and even as a slow-release fertilizer. However, further research is needed to verify whether PBC can simultaneously adsorb heavy metals in water without the risk of eutrophication but also passivate heavy metals and be applied as a slow-release fertilizer in soil. This is of great significance for promoting the green development of industry and the sustainable development of agriculture.

## 6. Conclusions

In conclusion, this paper provides a comprehensive review of the recent research progress on the preparation and applications of PBC and composite materials. The migration and transformation of phosphorus in biochar, alongside the impacts of various exogenous phosphorus sources, distinct carbonization processes, and parameters on the form and availability of phosphorus, were comprehensively discussed. Moreover, a comprehensive summary was provided regarding the environmental application of PBC in the adsorption of heavy metals in water. PBC demonstrates improved heavy metal adsorption performance compared to original biochar, showing strong stability and cyclic adsorption capabilities. It can effectively remediate heavy metal pollution in water bodies, including co-adsorption of multiple metals and specific adsorption for particular heavy metals in complex water environments. The principal mechanisms of adsorption encompass mineral precipitation, ion exchange, surface complexation, electrostatic interaction, physical adsorption, cation- $\pi$  interaction, and redox reactions.

**Author Contributions:** Conceptualization, Y.Z. and Y.L.; methodology, Y.Z.; writing—original draft preparation, Y.Z. and Y.L.; writing—review and editing, Y.Z., M.M. and H.C. All authors have read and agreed to the published version of the manuscript.

**Funding:** This study was supported by the Chongqing Graduate Scientific Research Innovation Project (CYB22212).

**Data Availability Statement:** Not applicable.

**Conflicts of Interest:** The authors declare no conflicts of interest.

## References

1. Xiang, M.; Li, Y.; Yang, J.; Li, Y.; Li, F.; Hu, B.; Cao, Y. Assessment of Heavy Metal Pollution in Soil and Classification of Pollution Risk Management and Control Zones in the Industrial Developed City. *Environ. Manag.* **2020**, *66*, 1105–1119. [[CrossRef](#)] [[PubMed](#)]
2. Vareda, J.; Valente, A.; Duraes, L. Assessment of heavy metal pollution from anthropogenic activities and remediation strategies: A review. *J. Environ. Manag.* **2019**, *246*, 101–118. [[CrossRef](#)] [[PubMed](#)]
3. Xie, S.; Yang, F.; Feng, H.; Wei, C.; Wu, F. Assessment of Potential Heavy Metal Contamination in the Peri-urban Agricultural Soils of 31 Provincial Capital Cities in China. *Environ. Manag.* **2019**, *64*, 366–380. [[CrossRef](#)] [[PubMed](#)]
4. Shikha, D.; Singh, P. In situ phytoremediation of heavy metal-contaminated soil and groundwater: A green inventive approach. *Environ. Sci. Pollut. Res.* **2021**, *28*, 4104–4124. [[CrossRef](#)] [[PubMed](#)]
5. Rana, A.; Sindhu, M.; Kumar, A.; Dhaka, R.; Chahar, M.; Singh, S.; Nain, L. Restoration of heavy metal-contaminated soil and water through biosorbents: A review of current understanding and future challenges. *Physiol. Plant.* **2021**, *173*, 394–417. [[CrossRef](#)] [[PubMed](#)]
6. Vidu, R.; Matei, E.; Predescu, A.M.; Alhalaili, B.; Pantilimon, C.; Tarcea, C.; Predescu, C. Removal of Heavy Metals from Wastewaters: A Challenge from Current Treatment Methods to Nanotechnology Applications. *Toxics* **2020**, *8*, 101. [[CrossRef](#)] [[PubMed](#)]
7. Gu, S.; Kang, X.; Wang, L.; Lichtfouse, E.; Wang, C. Clay mineral adsorbents for heavy metal removal from wastewater: A review. *Environ. Chem. Lett.* **2018**, *17*, 629–654. [[CrossRef](#)]
8. Fu, T.; Zhang, B.; Gao, X.; Cui, S.; Guan, C.Y.; Zhang, Y.; Zhang, B.; Peng, Y. Recent progresses, challenges, and opportunities of carbon-based materials applied in heavy metal polluted soil remediation. *Sci. Total Environ.* **2023**, *856*, 158810. [[CrossRef](#)]
9. Wang, J.; Wang, S. Preparation, modification and environmental application of biochar: A review. *J. Clean. Prod.* **2019**, *227*, 1002–1022. [[CrossRef](#)]
10. Xiang, W.; Zhang, X.; Chen, J.; Zou, W.; He, F.; Hu, X.; Tsang, D.; Ok, Y.S.; Gao, B. Biochar technology in wastewater treatment: A critical review. *Chemosphere* **2020**, *252*, 126539–126552. [[CrossRef](#)]
11. Bao, Z.; Feng, H.; Tu, W.; Li, L.; Li, Q. Method and mechanism of chromium removal from soil: A systematic review. *Environ. Sci. Pollut. Res.* **2022**, *29*, 35501–35517. [[CrossRef](#)] [[PubMed](#)]
12. Zhang, C.; Liu, L.; Zhao, M.; Rong, H.; Xu, Y. The environmental characteristics and applications of biochar. *Environ. Sci. Pollut. Res.* **2018**, *25*, 21525–21534. [[CrossRef](#)] [[PubMed](#)]
13. Huang, H.; Chen, Y.; Ma, R.; Luo, J.; Sun, S.; Lin, J.; Wang, Y. Preparation of high performance porous carbon by microwave synergistic nitrogen/phosphorus doping for efficient removal of Cu(2+) via capacitive deionization. *Environ. Res.* **2023**, *222*, 115342–115354. [[CrossRef](#)] [[PubMed](#)]
14. Cao, D.; Ji, Y.; Liu, L.; Li, L.; Li, L.; Feng, X.; Zhu, J.; Lu, X.; Mu, L. A facile and green strategy to synthesize N/P co-doped bio-char as VOCs adsorbent: Through efficient biogas slurry treatment and struvite transform. *Fuel* **2022**, *322*, 124156–124164. [[CrossRef](#)]
15. Ma, L.; Hu, X.; Liu, W.; Li, H.; Lam, P.; Zeng, R.; Yu, H. Constructing N, P-dually doped biochar materials from biomass wastes for high-performance bifunctional oxygen electrocatalysts. *Chemosphere* **2021**, *278*, 130508–130515. [[CrossRef](#)] [[PubMed](#)]
16. Kruse, A.; Zhang, T.; Becker, G.; Sachs, S.; He, X.; Xue, Q. The current phosphate recycling situation in China and Germany: A comparative review. *Front. Agric. Sci. Eng.* **2019**, *6*, 403–418. [[CrossRef](#)]
17. Zhang, F.; Zhang, K.; Li, G.; Zhang, W.; Zhang, T.; Hou, Y.; Ma, L.; Yuan, L.; Zhang, J.; Feng, G.; et al. Innovations of phosphorus sustainability: Implications for the whole chain. *Front. Agric. Sci. Eng.* **2019**, *6*, 321–332. [[CrossRef](#)]
18. Shao, J.; Gao, C.; Afi Seglah, P.; Xie, J.; Zhao, L.; Bi, Y.; Wang, Y. Analysis of the Available Straw Nutrient Resources and Substitution of Chemical Fertilizers with Straw Returned Directly to the Field in China. *Agriculture* **2023**, *13*, 1187. [[CrossRef](#)]
19. Rayne, N.; Aula, L. Livestock Manure and the Impacts on Soil Health: A Review. *Soil Syst.* **2020**, *4*, 64. [[CrossRef](#)]
20. Zhu, Y.; Zhao, Q.; Li, D.; Li, J.; Guo, W. Performance comparison of phosphorus recovery from different sludges in sewage treatment plants through pyrolysis. *J. Clean. Prod.* **2022**, *372*, 133728–133738. [[CrossRef](#)]
21. Müller-Stöver, D.; Jakobsen, I.; Grønlund, M.; Rolsted, M.; Magid, J.; Hauggaard-Nielsen, H.; Goss, M. Phosphorus bioavailability in ash from straw and sewage sludge processed by low-temperature biomass gasification. *Soil Use Manag.* **2018**, *34*, 9–17. [[CrossRef](#)]
22. Xiong, Q.; Wu, X.; Lv, H.; Liu, S.; Hou, H.; Wu, X. Influence of rice husk addition on phosphorus fractions and heavy metals risk of biochar derived from sewage sludge. *Chemosphere* **2021**, *280*, 130566–130576. [[CrossRef](#)] [[PubMed](#)]
23. Ghanim, B.; Kwapinski, W.; Leahy, J. Hydrothermal carbonisation of poultry litter: Effects of initial pH on yields and chemical properties of hydrochars. *Bioresour. Technol.* **2017**, *238*, 78–85. [[CrossRef](#)] [[PubMed](#)]
24. Kwapinski, W.; Kolinovic, I.; Leahy, J. Sewage Sludge Thermal Treatment Technologies with a Focus on Phosphorus Recovery: A Review. *Waste Biomass Valorization* **2021**, *12*, 5837–5852. [[CrossRef](#)]
25. Liu, W.J.; Li, W.W.; Jiang, H.; Yu, H.Q. Fates of Chemical Elements in Biomass during Its Pyrolysis. *Chem. Rev.* **2017**, *117*, 6367–6398. [[CrossRef](#)] [[PubMed](#)]
26. Huang, R.; Fang, C.; Lu, X.; Jiang, R.; Tang, Y. Transformation of Phosphorus during (Hydro)thermal Treatments of Solid Biowastes: Reaction Mechanisms and Implications for P Reclamation and Recycling. *Environ. Sci. Technol.* **2017**, *51*, 10284–10298. [[CrossRef](#)] [[PubMed](#)]
27. Peiris, C.; Alahakoon, Y.; Malaweera Arachchi, U.; Mlsna, T.; Gunatilake, S.; Zhang, X. Phosphorus-enriched biochar for the remediation of heavy metal contaminated soil. *J. Agric. Food Res.* **2023**, *12*, 100546–100553. [[CrossRef](#)]

28. Chen, G.; Wang, J.; Yu, F.; Wang, X.; Xiao, H.; Yan, B.; Cui, X. A review on the production of P-enriched hydro/bio-char from solid waste: Transformation of P and applications of hydro/bio-char. *Chemosphere* **2022**, *301*, 134646–134655. [[CrossRef](#)]
29. Arias, C.; da Silva, L.; Soares, M.; Forti, V. A bibliometric analysis on the agricultural use of biochar in Brazil from 2003 to 2021: Research status and promising raw materials. *Renew. Agric. Food Syst.* **2023**, *38*, e19. [[CrossRef](#)]
30. Wieczorek, D.; Zyszka-Haberecht, B.; Kafka, A.; Lipok, J. Determination of phosphorus compounds in plant tissues: From colourimetry to advanced instrumental analytical chemistry. *Plant Methods* **2022**, *18*, 22–38. [[CrossRef](#)]
31. Liu, F.; Xiao, Z.; Fang, J.; Li, H. Effect of Pyrolysis Treatment on Phosphorus Migration and Transformation of Pig, Cow and Sheep Manure. *Sustainability* **2023**, *15*, 9215. [[CrossRef](#)]
32. Bee, S.; Hamid, Z. Hydroxyapatite derived from food industry bio-wastes: Syntheses, properties and its potential multifunctional applications. *Ceram. Int.* **2020**, *46*, 17149–17175. [[CrossRef](#)]
33. Fang, Z.; Zhuang, X.; Zhang, X.; Li, Y.; Li, R.; Ma, L. Influence of parameters on the transformation behaviors and directional adjustment strategies of phosphorus forms during different thermochemical treatments of sludge. *Fuel* **2023**, *333*, 126544–126563. [[CrossRef](#)]
34. Yang, L.; Wu, Y.; Wang, Y.; An, W.; Jin, J.; Sun, K.; Wang, X. Effects of biochar addition on the abundance, speciation, availability, and leaching loss of soil phosphorus. *Sci. Total Environ.* **2021**, *758*, 143657. [[CrossRef](#)]
35. Chen, S.; Wang, J.; Wu, Z.; Deng, Q.; Tu, W.; Dai, G.; Zeng, Z.; Deng, S. Enhanced Cr(VI) removal by polyethylenimine- and phosphorus-codoped hierarchical porous carbons. *J. Colloid Interface Sci.* **2018**, *523*, 110–120. [[CrossRef](#)]
36. Mohamed, B.; Ellis, N.; Kim, C.; Bi, X. The role of tailored biochar in increasing plant growth, and reducing bioavailability, phytotoxicity, and uptake of heavy metals in contaminated soil. *Environ. Pollut.* **2017**, *230*, 329–338. [[CrossRef](#)]
37. Zhang, H.; Liao, W.; Zhou, X.; Shao, J.; Chen, Y.; Zhang, S.; Chen, H. Coeffect of pyrolysis temperature and potassium phosphate impregnation on characteristics, stability, and adsorption mechanism of phosphorus-enriched biochar. *Bioresour. Technol.* **2022**, *344*, 126273–126282. [[CrossRef](#)]
38. Yuan, Q.; Wang, P.; Wang, X.; Hu, B.; Wang, C.; Xing, X. Nano-chlorapatite modification enhancing cadmium(II) adsorption capacity of crop residue biochars. *Sci. Total Environ.* **2023**, *865*, 161097–161107. [[CrossRef](#)]
39. Chen, Y.; Li, M.; Li, Y.; Liu, Y.; Chen, Y.; Li, H.; Li, L.; Xu, F.; Jiang, H.; Chen, L. Hydroxyapatite modified sludge-based biochar for the adsorption of Cu(2+) and Cd(2+): Adsorption behavior and mechanisms. *Bioresour. Technol.* **2021**, *321*, 124413–124422. [[CrossRef](#)]
40. Yang, F.; Lv, J.; Zhou, Y.; Wu, S.; Sima, J. Co-pyrolysis of biomass and phosphate tailing to produce potential phosphorus-rich biochar: Efficient removal of heavy metals and the underlying mechanisms. *Environ. Sci. Pollut. Res.* **2023**, *30*, 17804–17816. [[CrossRef](#)]
41. Huang, K.; Hu, C.; Tan, Q.; Yu, M.; Shabala, S.; Yang, L.; Sun, X. Highly efficient removal of cadmium from aqueous solution by ammonium polyphosphate-modified biochar. *Chemosphere* **2022**, *305*, 135471–135478. [[CrossRef](#)] [[PubMed](#)]
42. Zhang, H.; Ke, S.; Xia, M.; Bi, X.; Shao, J.; Zhang, S.; Chen, H. Effects of phosphorous precursors and speciation on reducing bioavailability of heavy metal in paddy soil by engineered biochars. *Environ. Pollut.* **2021**, *285*, 117459–117469. [[CrossRef](#)] [[PubMed](#)]
43. Li, J.; He, F.; Shen, X.; Hu, D.; Huang, Q. Pyrolyzed fabrication of N/P co-doped biochars from (NH<sub>4</sub>)<sub>3</sub>PO<sub>4</sub>-pretreated coffee shells and appraisalment for remedying aqueous Cr(VI) contaminants. *Bioresour. Technol.* **2020**, *315*, 123840–123847. [[CrossRef](#)] [[PubMed](#)]
44. Huang, D.; Deng, R.; Wan, J.; Zeng, G.; Xue, W.; Wen, X.; Zhou, C.; Hu, L.; Liu, X.; Xu, P.; et al. Remediation of lead-contaminated sediment by biochar-supported nano-chlorapatite: Accompanied with the change of available phosphorus and organic matters. *J. Hazard. Mater.* **2018**, *348*, 109–116. [[CrossRef](#)] [[PubMed](#)]
45. Wang, Y.; Yu, L.; Yuan, H.; Ying, D.; Zhu, N. Improved removal of phosphorus from incinerated sewage sludge ash by thermochemical reduction method with CaCl<sub>2</sub> application. *J. Clean. Prod.* **2020**, *258*, 120779–120786. [[CrossRef](#)]
46. Gbouri, I.; Yu, F.; Wang, X.; Wang, J.; Cui, X.; Hu, Y.; Yan, B.; Chen, G. Co-Pyrolysis of Sewage Sludge and Wetland Biomass Waste for Biochar Production: Behaviors of Phosphorus and Heavy Metals. *Int. J. Environ. Res. Public Health* **2022**, *19*, 2818. [[CrossRef](#)] [[PubMed](#)]
47. Thomas, K.; Hamid, S.; Matthias, K.; Nils, S.; Marcus, Ö. Thermochemical equilibrium study of ash transformation during combustion and gasification of sewage sludge mixtures with agricultural residues with focus on the phosphorus speciation. *Biomass Convers. Biorefin.* **2021**, *11*, 57–68. [[CrossRef](#)]
48. Parthasarathy, P.; Al-Ansari, T.; Mackey, H.R.; Sheeba Narayanan, K.; McKay, G. A review on prominent animal and municipal wastes as potential feedstocks for solar pyrolysis for biochar production. *Fuel* **2022**, *316*, 123378–123392. [[CrossRef](#)]
49. Uchimiya, M.; Hiradate, S.; Antal, M. Dissolved Phosphorus Speciation of Flash Carbonization, Slow Pyrolysis, and Fast Pyrolysis Biochars. *ACS Sustain. Chem. Eng.* **2015**, *3*, 1642–1649. [[CrossRef](#)]
50. Xu, G.; Zhang, Y.; Shao, H.; Sun, J. Pyrolysis temperature affects phosphorus transformation in biochar: Chemical fractionation and 31P NMR analysis. *Sci. Total Environ.* **2016**, *569–570*, 65–72. [[CrossRef](#)]
51. Wang, S.; Zhang, H.; Huang, H.; Xiao, R.; Li, R.; Zhang, Z. Influence of temperature and residence time on characteristics of biochars derived from agricultural residues: A comprehensive evaluation. *Process Saf. Environ. Prot.* **2020**, *139*, 218–229. [[CrossRef](#)]

52. Li, J.; Li, Y.; Liu, F.; Zhang, X.; Song, M.; Li, R. Pyrolysis of sewage sludge to biochar: Transformation mechanism of phosphorus. *J. Anal. Appl. Pyrolysis* **2023**, *173*, 106065–106074. [[CrossRef](#)]
53. Fang, Z.; Liu, F.; Li, Y.; Li, B.; Yang, T.; Li, R. Influence of microwave-assisted pyrolysis parameters and additives on phosphorus speciation and transformation in phosphorus-enriched biochar derived from municipal sewage sludge. *J. Clean. Prod.* **2021**, *287*, 125550–125563. [[CrossRef](#)]
54. Li, J.; Dai, J.; Liu, G.; Zhang, H.; Gao, Z.; Fu, J.; He, Y.; Huang, Y. Biochar from microwave pyrolysis of biomass: A review. *Biomass Bioenergy* **2016**, *94*, 228–244. [[CrossRef](#)]
55. Chen, C.; Wei, R.; Shi, F.; Ma, X.; Zhou, X.; Xiong, Q. Analysis of the effects of prepyrolysis hydrothermal treatment on phosphorus recovery from sewage sludge using a life cycle assessment. *J. Clean. Prod.* **2022**, *377*, 134312–134319. [[CrossRef](#)]
56. Zhang, Y.; Yuan, H.; Cai, S.; Zhang, Y.; Wang, D.; Zhang, W. Molecular transformation pathway and bioavailability of organic phosphorus in sewage sludge under hydrothermal treatment: Importance of biopolymers interactions. *J. Clean. Prod.* **2023**, *385*, 135746–135754. [[CrossRef](#)]
57. Tangredi, A.; Barca, C.; Ferrasse, J.; Boutin, O. Effect of process parameters on phosphorus conversion pathways during hydrothermal treatment of sewage sludge: A review. *Chem. Eng. J.* **2023**, *463*, 142342–142358. [[CrossRef](#)]
58. Cui, X.; Yang, X.; Sheng, K.; He, Z.; Chen, G. Transformation of Phosphorus in Wetland Biomass during Pyrolysis and Hydrothermal Treatment. *ACS Sustain. Chem. Eng.* **2019**, *7*, 16520–16528. [[CrossRef](#)]
59. Xiong, J.; Pan, Z.; Xiao, X.; Huang, H.; Lai, F.; Wang, J.; Chen, S. Study on the hydrothermal carbonization of swine manure: The effect of process parameters on the yield/properties of hydrochar and process water. *J. Anal. Appl. Pyrolysis* **2019**, *144*, 104692–104701. [[CrossRef](#)]
60. Wang, H.; Yang, Z.; Li, X.; Liu, Y. Distribution and transformation behaviors of heavy metals and phosphorus during hydrothermal carbonization of sewage sludge. *Environ. Sci. Pollut. Res.* **2020**, *27*, 17109–17122. [[CrossRef](#)]
61. Shi, Y.; Chen, Z.; Zhu, K.; Fan, J.; Clark, J.; Luo, G.; Zhang, S. Speciation evolution and transformation mechanism of P during microwave hydrothermal process of sewage sludge. *Sci. Total Environ.* **2022**, *815*, 152801–152812. [[CrossRef](#)] [[PubMed](#)]
62. Soroush, S.; Ronsse, F.; Park, J.; Ghysels, S.; Wu, D.; Kim, K.; Heynderickx, P. Microwave assisted and conventional hydrothermal treatment of waste seaweed: Comparison of hydrochar properties and energy efficiency. *Sci. Total Environ.* **2023**, *878*, 163193–163205. [[CrossRef](#)] [[PubMed](#)]
63. Zhao, X.; Li, M.; Zhai, F.; Hou, Y.; Hu, R. Phosphate modified hydrochars produced via phytic acid-assisted hydrothermal carbonization for efficient removal of U(VI), Pb(II) and Cd(II). *J. Environ. Manag.* **2021**, *298*, 113487–113499. [[CrossRef](#)] [[PubMed](#)]
64. Hu, R.; Xiao, J.; Wang, T.; Chen, G.; Chen, L.; Tian, X. Engineering of phosphate-functionalized biochars with highly developed surface area and porosity for efficient and selective extraction of uranium. *Chem. Eng. J.* **2020**, *379*, 122388–122397. [[CrossRef](#)]
65. Deng, R.; Huang, D.; Wan, J.; Xue, W.; Lei, L.; Wen, X.; Liu, X.; Chen, S.; Yang, Y.; Li, Z.; et al. Chloro-phosphate impregnated biochar prepared by co-precipitation for the lead, cadmium and copper synergic scavenging from aqueous solution. *Bioresour. Technol.* **2019**, *293*, 122102–122109. [[CrossRef](#)] [[PubMed](#)]
66. Lyu, P.; Wang, G.; Wang, B.; Yin, Q.; Li, Y.; Deng, N. Adsorption and interaction mechanism of uranium (VI) from aqueous solutions on phosphate-impregnation biochar cross-linked Mg Al layered double-hydroxide composite. *Appl. Clay Sci.* **2021**, *209*, 106146–106157. [[CrossRef](#)]
67. Sun, Y.; Yuan, N.; Ge, Y.; Ye, T.; Yang, Z.; Zou, L.; Ma, W.; Lu, L. Adsorption behavior and mechanism of U(VI) onto phytic Acid-modified Biochar/MoS<sub>2</sub> heterojunction materials. *Sep. Purif. Technol.* **2022**, *294*, 121158–121169. [[CrossRef](#)]
68. Wang, C.; Wang, G.; Xie, S.; Dong, Z.; Zhang, L.; Zhang, Z.; Song, J.; Deng, Y. Phosphorus-rich biochar modified with *Alcaligenes faecalis* to promote U(VI) removal from wastewater: Interfacial adsorption behavior and mechanism. *J. Hazard. Mater.* **2023**, *454*, 131484. [[CrossRef](#)]
69. Tang, Z.; Dai, Z.; Gong, M.; Chen, H.; Zhou, X.; Wang, Y.; Jiang, C.; Yu, W.; Li, L. Efficient removal of uranium(VI) from aqueous solution by a novel phosphate-modified biochar supporting zero-valent iron composite. *Environ. Sci. Pollut. Res.* **2023**, *30*, 40478–40489. [[CrossRef](#)]
70. Fan, Y.; Wang, H.; Deng, L.; Wang, Y.; Kang, D.; Li, C.; Chen, H. Enhanced adsorption of Pb(II) by nitrogen and phosphorus co-doped biochar derived from *Camellia oleifera* shells. *Environ. Res.* **2020**, *191*, 110030–110040. [[CrossRef](#)]
71. Wang, Q.; Duan, C.; Xu, C.Y.; Geng, Z. Efficient removal of Cd(II) by phosphate-modified biochars derived from apple tree branches: Processes, mechanisms, and application. *Sci. Total Environ.* **2022**, *819*, 152876–152887. [[CrossRef](#)] [[PubMed](#)]
72. Chen, Y.; Ning, P.; Miao, R.; He, L.; Guan, Q. Resource utilization of agricultural residues: One-step preparation of biochar derived from *Pennisetum giganteum* for efficiently removing chromium from water in a wide pH range. *Environ. Sci. Pollut. Res.* **2021**, *28*, 69381–69392. [[CrossRef](#)] [[PubMed](#)]
73. Chen, X.; Wang, Y.; Xia, H.; Ren, Q.; Li, Y.; Xu, L.; Xie, C.; Wang, Y. “One-can” strategy for the synthesis of hydrothermal biochar modified with phosphate groups and efficient removal of uranium(VI). *J. Environ. Radioact.* **2023**, *263*, 107182–107194. [[CrossRef](#)] [[PubMed](#)]
74. Cui, X.; Fang, S.; Yao, Y.; Li, T.; Ni, Q.; Yang, X.; He, Z. Potential mechanisms of cadmium removal from aqueous solution by *Canna indica* derived biochar. *Sci. Total Environ.* **2016**, *562*, 517–525. [[CrossRef](#)] [[PubMed](#)]
75. Zhang, Z.; Li, Y.; Zong, Y.; Yu, J.; Ding, H.; Kong, Y.; Ma, J.; Ding, L. Efficient removal of cadmium by salts modified-biochar: Performance assessment, theoretical calculation, and quantitative mechanism analysis. *Bioresour. Technol.* **2022**, *361*, 127717–127728. [[CrossRef](#)] [[PubMed](#)]

76. Ge, Q.; Tian, Q.; Wang, S.; Zhang, J.; Hou, R. Highly Efficient Removal of Lead/Cadmium by Phosphoric Acid-Modified Hydrochar Prepared from Fresh Banana Peels: Adsorption Mechanisms and Environmental Application. *Langmuir* **2022**, *38*, 15394–15403. [[CrossRef](#)] [[PubMed](#)]
77. Sun, L.; Gong, P.; Sun, Y.; Qin, Q.; Song, K.; Ye, J.; Zhang, H.; Zhou, B.; Xue, Y. Modified chicken manure biochar enhanced the adsorption for Cd<sup>2+</sup> in aqueous and immobilization of Cd in contaminated agricultural soil. *Sci. Total Environ.* **2022**, *851*, 158252–158260. [[CrossRef](#)]
78. Wang, Y.; Li, H.; Lin, S. Advances in the Study of Heavy Metal Adsorption from Water and Soil by Modified Biochar. *Water* **2022**, *14*, 3894. [[CrossRef](#)]
79. Xu, Y.; Bai, T.; Li, Q.; Yang, H.; Yan, Y.; Sarkar, B.; Lam, S.S.; Bolan, N. Influence of pyrolysis temperature on the characteristics and lead(II) adsorption capacity of phosphorus-engineered poplar sawdust biochar. *J. Anal. Appl. Pyrolysis* **2021**, *154*, 105010. [[CrossRef](#)]
80. Liu, X.; Yin, H.; Liu, H.; Cai, Y.; Qi, X.; Dang, Z. Multicomponent adsorption of heavy metals onto biogenic hydroxyapatite: Surface functional groups and inorganic mineral facilitating stable adsorption of Pb(II). *J. Hazard. Mater.* **2023**, *443*, 130167–130177. [[CrossRef](#)]
81. Zhou, X.; Xu, D.; Yang, J.; Yan, Z.; Zhang, Z.; Zhong, B.; Wang, X. Treatment of distiller grain with wet-process phosphoric acid leads to biochar for the sustained release of nutrients and adsorption of Cr(VI). *J. Hazard. Mater.* **2023**, *441*, 129949. [[CrossRef](#)] [[PubMed](#)]
82. Xiao, Y.; Xue, Y.; Gao, F.; Mosa, A. Sorption of heavy metal ions onto crayfish shell biochar: Effect of pyrolysis temperature, pH and ionic strength. *J. Taiwan Inst. Chem. Eng.* **2017**, *80*, 114–121. [[CrossRef](#)]
83. Wang, C.; Wang, G.; Xie, S.; Wang, J.; Guo, Y. Removal behavior and mechanisms of U(VI) in aqueous solution using aloe vera biochar with highly developed porous structure. *J. Radioanal. Nucl. Chem.* **2022**, *331*, 2273–2283. [[CrossRef](#)]
84. Shi, T.; Jia, S.; Chen, Y.; Wen, Y.; Du, C.; Guo, H.; Wang, Z. Adsorption of Pb(II), Cr(III), Cu(II), Cd(II) and Ni(II) onto a vanadium mine tailing from aqueous solution. *J. Hazard. Mater.* **2009**, *169*, 838–846. [[CrossRef](#)] [[PubMed](#)]
85. Chu, G.; Zhao, J.; Huang, Y.; Zhou, D.; Liu, Y.; Wu, M.; Peng, H.; Zhao, Q.; Pan, B.; Steinberg, C.E.W. Phosphoric acid pretreatment enhances the specific surface areas of biochars by generation of micropores. *Environ. Pollut.* **2018**, *240*, 1–9. [[CrossRef](#)] [[PubMed](#)]
86. Zhang, H. *Coordination Chemistry: Principles and Applications*; Chemical Industry Press: Beijing, China, 2008; pp. 334–335.
87. Yi, W. *Research on Heavy Metal Removal from Stormwater Runoff in Constructed Wetlands with Media of Zeolite*; Zhejiang University: Hangzhou, China, 2015.
88. Li, X. *Remediation of Cd and Ni Contaminated Soil by Cattle-Manure-Derived Biochar and Zeolite*; Huazhong Agricultural University: Wuhan, China, 2017.
89. Zhao, G.; Zhu, H. Cation- $\pi$  Interactions in Graphene-Containing Systems for Water Treatment and Beyond. *Adv. Mater.* **2020**, *32*, 1905756–1905777. [[CrossRef](#)] [[PubMed](#)]
90. Harvey, O.; Herbert, B.; Rhue, R.; Kuo, L. Metal interactions at the biochar-water interface: Energetics and structure-sorption relationships elucidated by flow adsorption microcalorimetry. *Environ. Sci. Technol.* **2011**, *45*, 5550–5556. [[CrossRef](#)]
91. Zhao, J.; Wang, L.; Chu, G. Comparison of the Sorption of Cu(II) and Pb(II) by Bleached and Activated Biochars: Insight into Complexation and Cation- $\pi$  Interaction. *Agronomy* **2023**, *13*, 1282. [[CrossRef](#)]
92. Chen, M.; He, F.; Hu, D.; Bao, C.; Huang, Q. Broadened operating pH range for adsorption/reduction of aqueous Cr(VI) using biochar from directly treated jute (*Corchorus capsularis* L.) fibers by H<sub>3</sub>PO<sub>4</sub>. *Chem. Eng. J.* **2020**, *381*, 122739–122748. [[CrossRef](#)]
93. Yi, Y.; Wang, X.; Zhang, Y.; Yang, K.; Ma, J.; Ning, P. Formation and mechanism of nanoscale zerovalent iron supported by phosphoric acid modified biochar for highly efficient removal of Cr(VI). *Adv. Powder Technol.* **2023**, *34*, 103826–103838. [[CrossRef](#)]

**Disclaimer/Publisher's Note:** The statements, opinions and data contained in all publications are solely those of the individual author(s) and contributor(s) and not of MDPI and/or the editor(s). MDPI and/or the editor(s) disclaim responsibility for any injury to people or property resulting from any ideas, methods, instructions or products referred to in the content.